A Study of Biodiesel and Biodiesel Petroleum Diesel Blends to Mitigate Filter Blocking

James Barker, Jaqueline Reid, and Edward Wilmot
Innospec

Anastarsia Carter, John Langley and Julie Herniman
University of Southampton

ABSTRACT

There are many anthropogenic climate change mitigation strategies being adopted worldwide. One of these is the adoption of biodiesel FAME (Fatty Acid Methyl Ester), in transportation. The fuel has been widely promoted as replacement for petroleum diesel because of its potential benefits for life cycle greenhouse gas emissions, carbon dioxide reduction and particulate matter improvements.

Presently biodiesel may be made from a wide variety of starting materials, including food waste and agricultural materials such as vegetable oils and greases. The number and variety of possible starting materials continues to increase. Though, there is a limiting factor in the use of FAME, and that is cold weather operability. The regional climate can often influence FAME adoption with resultant economic and environmental implications. Often this cold temperature operability manifests itself as in vehicle fuel filter blocking. Several analytical protocols have been produced over the last few years to identify the chemicals in biodiesel that cause this problem. However, the presence of petroleum hydrocarbons compromises many of these methods and others involve derivatization. Here we propose a protocol built around supercritical fluid chromatography mass spectrometry (SFC-MS) and Fourier transform ion cyclotron mass spectrometry (FT-ICR MS) that has the flexibility to meet these challenges and allow the analysis of petroleum diesel/FAME blends and afford detection of the suspect compounds causing filter blocking under cold temperature

INTRODUCTION

The use of FAME worldwide and blends with petrodiesel has resulted in incidents regarding filter blocking. In many cases information regarding composition of the FAME and its impurities [1] would allow blenders to understand and manage the possible climatic problems they may experience. The subject has seen numerous historical and recent studies Csontos *et al.* have published several papers related to the analysis of FAME impurity blocked fuel filters [2,3,4]. Barker *et al.* have also investigated biodiesel impurities on filters [5,6]. Fersner *et al.* [7] used the standard method ASTM D2068 [8] filter blocking tendency to investigate biodiesel impurity filter blocking. Jolly also found the impurities in biodiesel caused filter blocking in field samples [9], and Gopalan [10] showed the importance of degradation products. Barker [11] and Richards [12] identified biodiesel origin acids on filters, and recent work by Heiden [13] has introduced a cooling step to known analytical protocols to help with interferences found when petrodiesel is present. The work regarding filter blocking incidents has led to specifications for biofuels EN14214:2019[14] and ASTM D6751-23a [15] being tightened and new methods developed to analyze impurity componentry in biodiesel, for example saturated monoglycerides by gas chromatography EN17057 [16], but the majority of methods cannot be used for a petrodiesel/biodiesel blend. This lack of methodologies is a severe limitation to those seeking to blend in certain climatic circumstances. The analytical technique of mass spectrometry is well suited to this task and a new rapid methodology will be described herein utilizing supercritical fluid chromatography-mass spectrometry, accurate mass measurement and tandem mass spectrometry.

METHODS AND SAMPLES

Samples:

A selection of nine petrodiesel/biodiesel samples from the diesel pool were sourced from the field. The fuels were all hydrocarbon biodiesel blends from Europe, USA, and Scandinavia, except diesel 1 which was 100% commercial biodiesel. FAMEs were observed to be present in all nine fuels during analysis, with all diesels containing FAMEs C18:3, C18:2, and C18:1.

The major differences observed in FAME makeup: In diesel 1, diesel 2, diesel 3 and diesel 5

(C16:1;C16:0;C18:0) were observed. An absence of C16 FAMEs were observed in diesel 4, diesel 5, diesel 6, diesel 8 and diesel 9. An absence of FAME C18:0 was observed in diesel 6 and diesel 7.

Methods:

The samples were analyzed by positive and negative ion electrospray ionization (ESI) ultra high performance supercritical fluid chromatography mass spectrometry (UHPSFC-MS) and positive ion electrospray ionization Fourier transform ion cyclotron resonance mass spectrometry, (FT-ICR-ESI+MS). In the former case samples were introduced undiluted. In the latter a toluene solvent mix was used followed by dilution until a data intensity of 10^8 was noted in the mass spectrometer. The sample preparation and dilution were optimized to negate problems associated with space charge effects.

Instruments:

Note the mass spectral and other techniques have been described in detail previously in other SAE papers [17,18].

UHPSFC-MS

Analyses were undertaken using an Acquity UPC^2 system (Waters, Manchester, U.K.) coupled to a Waters SQD2 (Waters, Manchester, U.K.) single quadrupole mass spectrometer. Tandem MS analyses were undertaken using an Acquity UPC^2 system (Waters, Manchester, U.K.) coupled to a Waters Xevo TQD (Waters, Manchester, U.K.) triple quadrupole mass spectrometer. Using positive ion ESI-UHPSFC-MS ammonium acetate was added to the methanol make-up flow to preferentially form the ammoniated adduct $[M + NH_4]^+$ when analyzing the sample by positive ion electrospray mass spectrometry.

FT-ICR MS

The high resolution mass spectrometry (HR-MS) analyses were acquired using a Fourier transform Ion Cyclotron Resonance Mass Spectrometer (FT-ICR MS) (Bruker Daltonics, Coventry, U.K.). with a 4.7 Tesla magnet. An ESI source was used with a TD (Time Domain) of 2M and 64 scans. Sodiated molecules $[M + Na]^+$ were the abundant ions when using direct infusion positive ion ESI FT-ICR MS.

ANALYSIS

The following known climatically induced filter deposit forming compounds were highlighted for analysis

- Fatty acid methyl esters (FAMEs)

- Fatty acid methyl ester (FAME) oxidation products

- Free fatty acids (FFAs)

- Sterol glucosides (SGs)

- Monoacylglycerols (MAGs)

One example of each compound found to be present within the fuel will be shown in detail, using positive and negative ion UHPSFC-MS and FT-ICR MS data. A typical example base peak ion current chromatogram (BPICC) is shown in Figure 1 and the relevant areas of interest described. The reconstructed ion current chromatograms (RICCs) of each impurity of interest are described under each impurity subheading.
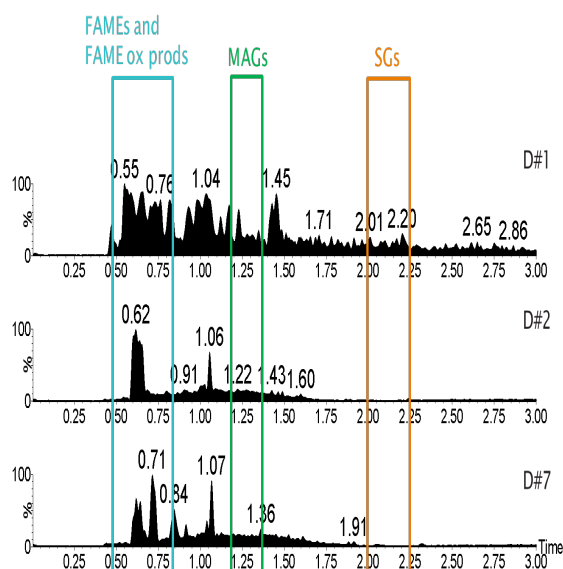

Figure 1   Positive ion ESI BPICCs of diesel samples 1, 2 and 7 with retention time regions (minutes) highlighted for compounds of interest.

Fatty Acid Methyl Esters (FAMES)

FAMEs have been linked to filter blocking and deposit formation [18,19].Table 1 shows a summary of FAMEs to be screened for, their respective molecular formulae and structures, adducts that can be present and their associated masses. Nominally isobaric species are in bold and underlined.

Table 1 FAME Molecular formulae and masses.

FAMEs (Carbon number: number of double bonds)	Molecular formula, exact mass and structure	Expected m/z (nominal for UHPSFC-MS, monoisotopic (4 dp) for FT-ICR MS)		
		[M + H]+	[M + NH4]+	[M + Na]+
C16:1	$C_{17}H_{32}O_2$, 268.24 g/mol	269.2475	286 (tR:0.58 min)	291.2301
C16:0	$C_{17}H_{34}O_2$, 270.26 g/mol	271.2636	288 (tR:0.60 min)	293.2456
C18:3	$C_{19}H_{32}O_2$, 292.24 g/mol	293.2480	310 (tR:0.60 min)	315.2295
C18:2	$C_{19}H_{34}O_2$, 294.26 g/mol	295.2636	312 (tR:0.62 min)	317.2451
C18:1	$C_{19}H_{36}O_2$, 296.27 g/mol	297.2791	314 (tR:0.64 min)	319.2608
C18:0	$C_{19}H_{38}O_2$, 298.29 g/mol	299.2945	316 (tR:0.68 min)	321.2765

The diesel fuel number 1 will be used to illustrate this class of analysis. FAMEs were found to elute at tR 0.55-0.70 min as shown in Figure 2 (positive ion ESI UHPSFC-MS) base peak ion current chromatogram (BPICC) of diesel 1. The corresponding positive ion UHPSFC-ESI mass spectrum shown in Figure 3, shows ammoniated molecules [M + NH4]+ observed at nominal m/z 286-316 that are consistent with compounds of nominal mass 268-298 g/mol and are in agreement with nominal masses of FAMEs from literature [20].
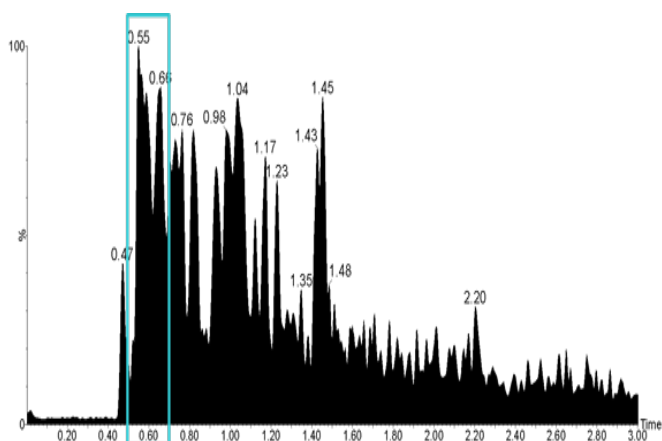

Figure 2 Positive ion ESI UHPSFC-MS BPICC of diesel 1 with pale blue box highlighting FAMEs region of retention (tR 0.55-0.70 min.).
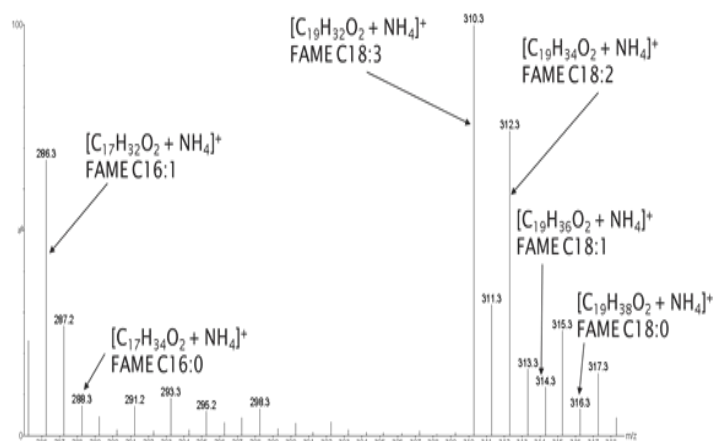

Figure 3 Positive ion ESI UHPSFC mass spectrum of diesel 1 at tR 0.55-0.70 min, zoomed range m/z 285-319.

RICCs of associated m/z values for FAMEs ([M + NH4]+ as shown in Table 1 are shown in Figure 4. The peaks observed are highly consistent with C16:1, C16:0, C18:3, C18:2, C18:1 and C18:0 FAMEs. Chromatographic separation of the positive ion ESI UHPSFC-MS method provides both separation of the FAMES by chain length as well as by degree of saturation.
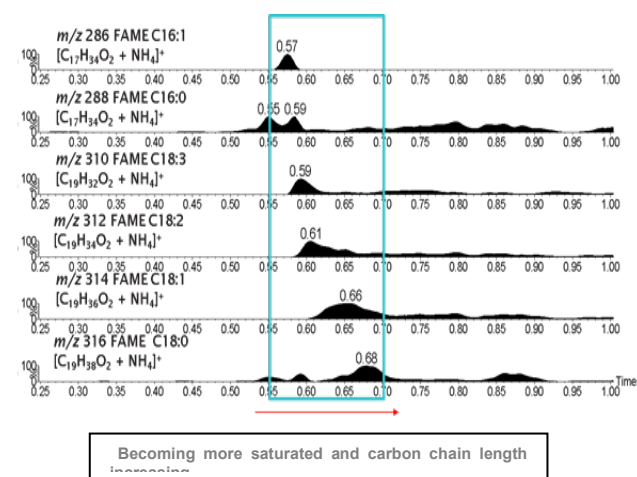

Figure 4 Positive ion ESI UHPSFC-MS RICCs of diesel 1 showing FAMEs with pale blue box highlighting FAMEs region of retention (tR 0.55-0.70 min.).

Figure 5 shows sodiated molecules observed for FAMEs C16:1, C16:0, C18:3, C18:2, C18:1 and C18:0 when using direct infusion positive ion ESI FT-ICR MS (Table 1).This is in agreement with proposed FAMEs observed in the positive ion ESI UHPSFC-MS data for diesel 1 with the sodium adducts further confirming presence of FAME species with accurate mass measurements.
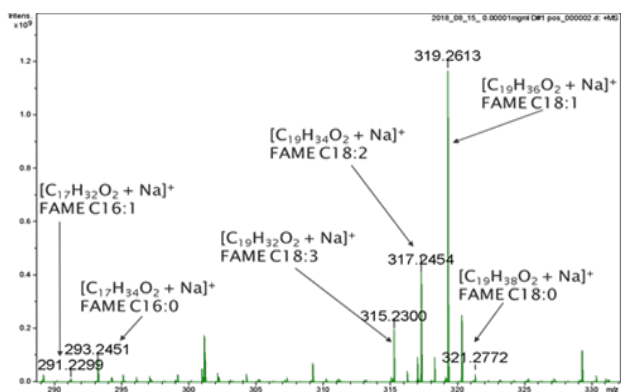
Figure 5 Direct infusion positive ion ESI FT-ICR mass spectrum of diesel 1 (zoomed *m/z* 290-330), showing sodiated molecules for FAMEs.

In summary, FAMEs were observed to be present in all nine fuels during analysis, with all diesels containing FAMEs C18:3, C18:2, and C18:1. The differences observed were an absence of C16 Fame in diesels 4, 5, 6,8, and 9. There was also an absence of FAME C18:0 in diesel 6 and 7.

Fatty Acid Methyl Esters (FAME) oxidation products

FAMEs are known to have low stability and are very susceptible to auto oxidation [21,22] and they linked to filter blocking [18,23,24].Table 2 shows a summary of the FAMEs and FAME oxidation products, their respective molecular formulae, adducts that can be present and their associated masses [25]. Each FAME has a designated color, dependent on number of double bonds, which match the colored arrows in figures 6 and 9 and it should be noted only C18 FAME oxidation products were highlighted in this study. Clearly others could be analyzed using the same protocol. Diesel 5 was used to illustrate this product. The sample showed that multiple species have the same nominal mass, as the FAME oxidation products. In the positive ion ESI UHPSFC-MS data, multiple peaks at various retention times are observed for these species in RICCs. This makes it difficult to assign peaks with confidence even if expected retention time known. Whereas direct infusion positive ion ESI FT-ICR MS provides separation of nominally isobaric species due to accurate mass measurements, providing molecular formulae. Therefore, direct infusion positive ion ESI FT-ICR MS is the preferred technique for FAME oxidation products in petrodiesel/biodiesel blends and will be shown first with positive ion ESI UHPSFC-MS discussed afterwards.

Table 2 FAME oxidation products molecular formulae and masses.

FAMEs (carbon number: number of double bonds)	Molecular formula	Expected *m/z* (nominal for UHPSFC-MS, monoisotopic for FT-ICR MS)								
		$[M+H]^+$	$[M+NH_4]^+$	$[M+Na]^+$	$[(M+O)+NH_4]^+$	$[(M+O)+Na]^+$	$[(M+2O)+NH_4]^+$	$[(M+2O)+Na]^+$	$[(M+3O)+NH_4]^+$	$[(M+3O)+Na]^+$
C18:3	$C_{19}H_{32}O_2$	293.248	310	315.23	326	331.225	342	347.2197	358	363.2147
C18:2	$C_{19}H_{34}O_2$	295.263	312	317.246	328	333.24	344	349.2354	360	365.2307
C18:1	$C_{19}H_{36}O_2$	297.279	314	319.262	330	335.256	346	351.2506	362	367.246

However, it should be noted that positive ion ESI FT-ICR MS will only show one species at a given *m/z* and not show structural isomer information, although it can be used in conjunction with chromatographic separation in the positive ion ESI FT-ICR MS method. Figure 6 shows ions consistent with the respective FAME oxidation products up to the addition of three addition oxygen atoms in agreement with ions shown in Table 2.
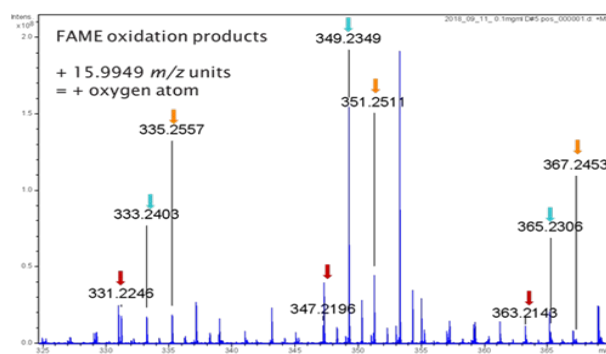

Figure 6 Direct Infusion positive ion ESI-FT-ICR mass spectrum of diesel 5 range *m/z* 325-370 showing sodiated products for C18 FAME oxidation products up to the addition of three oxygen atoms.

FAMEs and FAME oxidation products were found to elute between t_R 0.50-0.80 min as shown in Figure 7. The corresponding positive ion ESI UHPSFC mass spectrum shown in Figure 8 shows ammoniated molecules $[M + NH_4]^+$ observed at nominal *m/z* 310-360, which are consistent with compounds of nominal mass 293-343 g/mol, which is in agreement with FAMEs and FAME oxidation product nominal masses as shown in Table2.
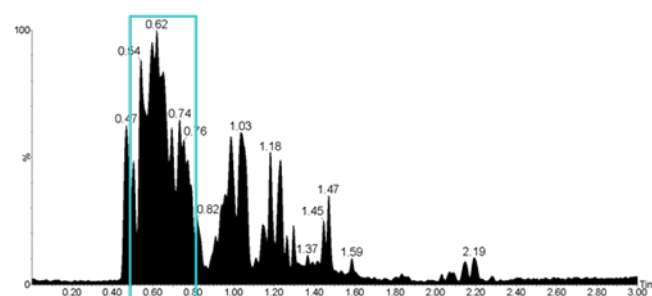

Figure 7 Positive ion ESI UHPSFC-MS BPICC of diesel5 with pale

blue box highlighting FAMEs and C18 FAME oxidation products region of retention (t_R 0.50 -0.80 min.).
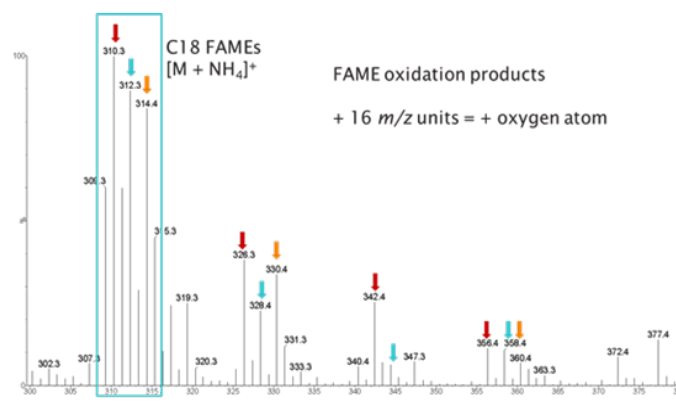

Figure 8 Positive ion ESI UHPSFC mass spectrum of diesel5 at t_R 0.50-0.80 min (zoomed range *m/z* 300-380), showing ammoniated molecules for C18 FAMEs and their respective FAME oxidation products, up to the addition of three oxygens.

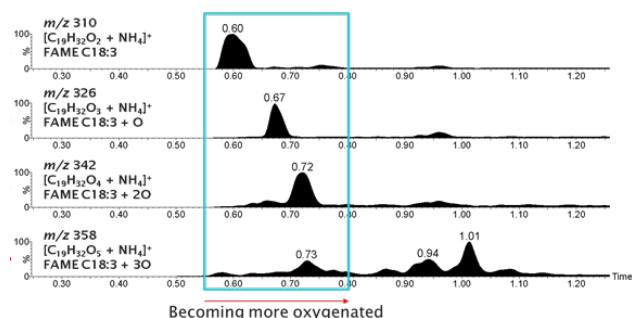RICCs for nominal *m/z* associated with FAME C18:3 and associated FAME oxidation products (in this case [M + NH₄]⁺ as shown in Table 2 and confirms the assignment. Figure 9.

Figure 9 Positive ion ESI UHPSFCMS RIICs of diesel 5 showing 18:3 FAME and FAME Oxidation products.

FAME oxidation products show that diesels have been oxidized, suggesting for example poor storage or old fuel. The difference in abundances of FAME oxidation products as well as the number of oxygen atoms observed corresponds to the different extent of oxidation each fuel has undergone.
Both techniques used were suitable for FAME oxidation products analysis however positive ion ESI FT-ICR MS was able to confirm the assignment and a molecular formula. In summary, C18 FAME oxidation products were only observed to be present in diesels 1, 2, 3, 4, 5, 7 and 9 during analysis. C18 FAME oxidation products were found to be absent in diesel 6 and 8 suggesting that these fuels contain unoxidized FAMEs.

FREE FATTY ACIDS (FFAs)

FFAs are well known as a contributing compound for metal carboxylates deposits both in fuel filter and fuel injector IDIDs [19,23,26]. Diesel 8 will be used to illustrate this group of compounds. FFAs were found

to elute at t_R 0.85 – 1.20 min as shown in Figure 10.The corresponding negative ion ESI UHPSFC mass spectrum shown in Figure 11 shows deprotonated molecules [M – H]⁻ observed at nominal *m/z* values matching those in Table 3. RICCs of associated *m/z* values for FFAs (in this case [M – H]⁻ as shown in Figure12 were used for compound confirmation as

Table 3 Free acids molecular formulae and masses

¤	¤	*m/z*² (nominal for UHPSFC-MS, monoisotopic for FT-ICR MS)¤
FFA¶ (Carbon number:number of double-bonds)¤	Molecular·formula,·exact·mass·and·structure¤	[M-·H]-¤
C14:0¤	C₁₄H₂₈O₂, 228.21·g/mol¶	227.2022¶ (t_R:0.96·min)¤
C16:1¤	C₁₆H₃₀O₂, 254.22·g/mol¶	253.2180¶ (t_R:1.02·min)¤
C16:0¤	C₁₆H₃₂O₂, 256.24·g/mol¶	255.2337¶ (t_R:1.05·min)¤
C18:3¤	C₁₈H₃₀O₂, 278.22·g/mol¶	277.2182¶ (t_R:1.03·min)¤
C18:2¤	C₁₈H₃₂O₂, 280.24·g/mol¶	279.2339¶ (t_R:1.04·min)¤
C18:1¤	C₁₈H₃₄O₂, 282.26·g/mol¶	281.2496¶ (t_R:1.09·min)¤
C18:0¤	C₁₈H₃₆O₂, 284.27·g/mol¶	283.2652¶ (t_R:1.14·min)¤

shown in Table 3, and the peaks observed suggest the presence of C14:0, C16:1, C16:0, C18:3, C18:2, C18:1 and C18:0 FFAs. Additionally, chromatographic separation of the negative ion ESI UHPSFC-MS method provided both separation of the FFAs by chain length as well as by degree of saturation.
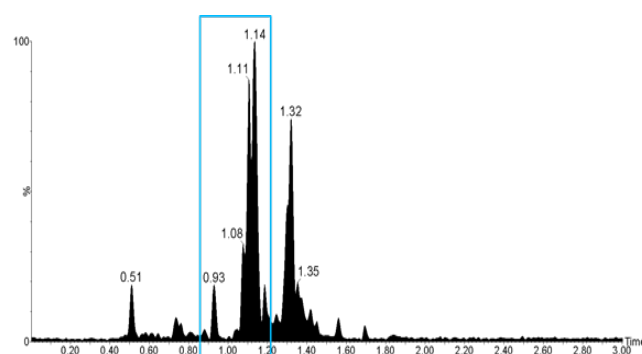

Figure 10 Negative ion ESIUHPSFC-MS BPICC of diesel 8, pale blue box highlighting FFAs region of retention (t_R 0.85-0.2min.).
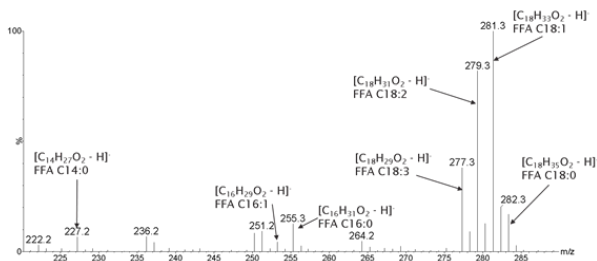
Figure 11 Negative ion ESI UHPSFC mass spectrum of diesel 8 at t_R 0.85-1.20 min (range m/z 220-290).
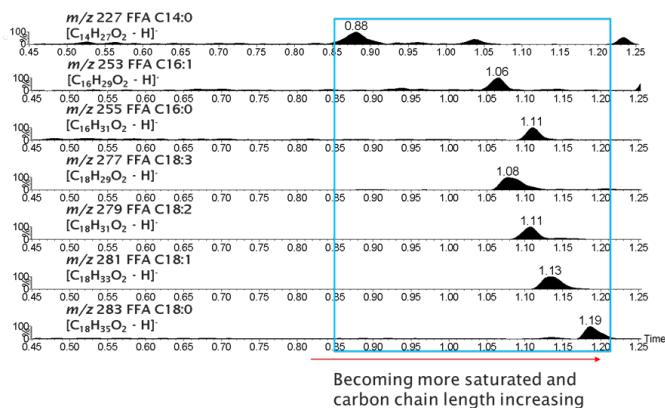

Figure 12 Negative ion ESI UHPSFC-MS RICCs of diesel 8 showing FFAs (t_R 0.85-1.20m min.).

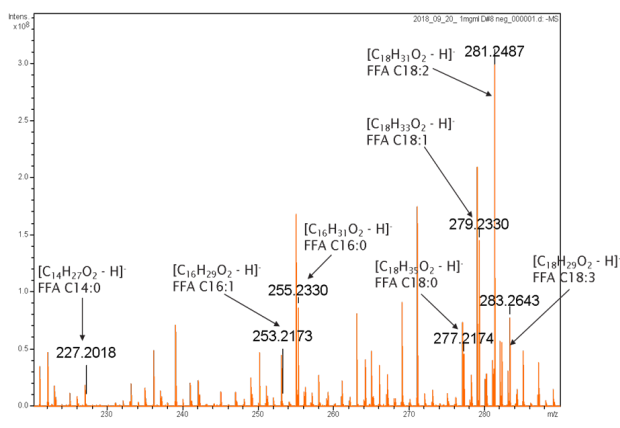The FFAs were also observed as deprotonated molecules [M - H]$^-$ in diesel 8 (m/z values in Figure 13.

Figure 13- Direct infusion negative ion ESI FT-ICR mass spectrum of diesel 8 (zoomed range m/z 220-290), showing deprotonated molecules for FFAs**.**

Using direct infusion negative ion ESI FT-ICR MS. The accurate mass data provides further confidence that C14:0, C16:1, C16:0, C18:3, C18:2, C18:1 and C18:0 FFAs were observed in diesel in agreement with negative ion ESI UHPSFC-MS. In summary FFAs were observed to be present in all nine diesel samples. The major differences noted were diesel 2 and 7 only have confirmed assignments for FFAs C18:1 and C18:2.FFA C16:1 is only confirmed to be present in diesels 3, 4, 8 and 9 with tentative assignments for diesels 5 and 6.

They key similarities are FFAs C18:2 and C18:1 are present in all nine diesels. FFAs C18:0, C18:3 and C16:3 are present in all diesels except 2 and 7.

MONOGLYCEROLS (MAGs)

Monoacylglycerols (MAGs) consist of a glycerol linked *via* an ester bond to a fatty acid [27]. MAGs are present as minor constituents or contaminants, within biodiesel as a by-product of incomplete transesterification [28].

Saturated MAGs have been found to plug fuel filters due to the low solubility of MAGs in biodiesel leading to the formation of solid precipitates in cold weather [29-31].

Table 4 shows a summary of the MAGs, their respective molecular formulae and structures, adducts that can be present and their associated masses [32] with nominally isobaric species m/z in bold and underlined.

Table 4 MAGs molecular formulae and masses

MAGs (Carbon number: number of double bonds)	Molecular formula, exact mass and structure	Expected m/z (nominal for SFC, monoisotopic (4 dp) for FT)		
		[M + H]$^+$	[M + NH$_4$]$^+$	[M + Na]$^+$
C16:0	$C_{19}H_{38}O_4$, 330.28 g/mol	331.2843	348 (t_R: 1.25 min)	__353.2662__
C18:3	$C_{21}H_{36}O_4$, 352.26 g/mol	__353.2686__	370 (t_R: 1.23 min)	375.2506
C18:2	$C_{21}H_{38}O_4$, 354.28 g/mol	355.2843	372 (t_R: 1.25 min)	377.2662
C18:1	$C_{21}H_{40}O_4$, 356.29 g/mol	357.2999	374 (t_R: 1.28 min)	379.2819
C18:0	$C_{21}H_{42}O_4$, 358.31 g/mol	359.3156	376 (t_R: 1.31 min)	381.2975

Diesel 3 is the example used to illustrate the MAGs within diesels identification.

MAGs were found to elute at t_R 1.20-1.35 min. as shown in Figure 14. The corresponding positive ion ESI UHPSFC mass spectrum shown in Figure 15 shows a mixture of protonated [M + H]$^+$ and ammoniated [M + NH$_4$]$^+$ molecules with nominal masses in agreement with MAGs nominal masses in Table 4.
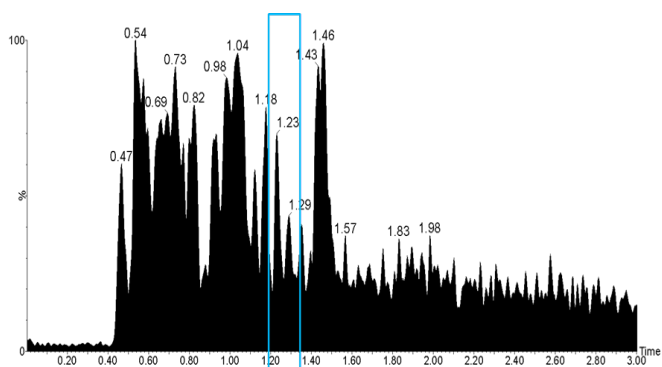
Figure 14 Positive ion ESI UHPSFC-MS BPICC of diesel 9 with pale blue box highlighting MAGs region of retention (t_R 1.20-1.35 min.).
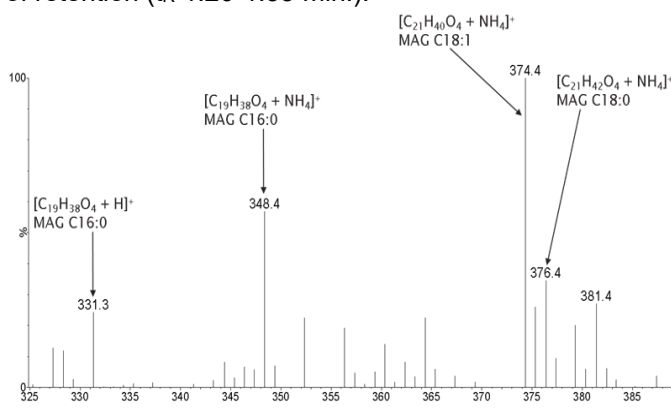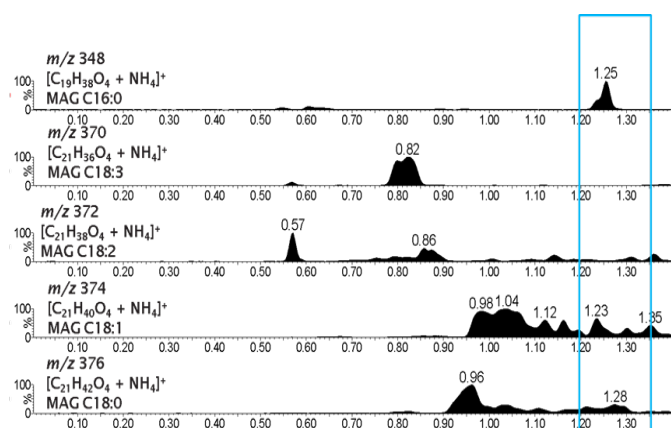

Figure 15 Positive ion ESI UHPSFC mass spectrum of diesel 9 at t_R 1.20-1.35 min (zoomed range m/z 325-390).

RICCs of associated m/z values for MAGs [M + NH$_4$]$^+$ as shown in Figure 16 which supports that the respective peaks are related to MAGs C16:0, C18:3, C18:2, C18:1 and C18:0, and is in agreement with those observed in the direct infusion positive ion ESI FT-ICR MS data.

Figure 16 Positive ion ESI UHPSFC-MS RICCs of diesel9 showing MAGs with pale blue box highlighting MAGs region of retention (t_R 1.20-1.35 min.).

For additional confirmation and to aid separation of nominally isobaric species, MAGs are observed as sodiated molecules [M + Na]$^+$ using direct infusion positive ion ESI FT-ICR MS, Figure 17.
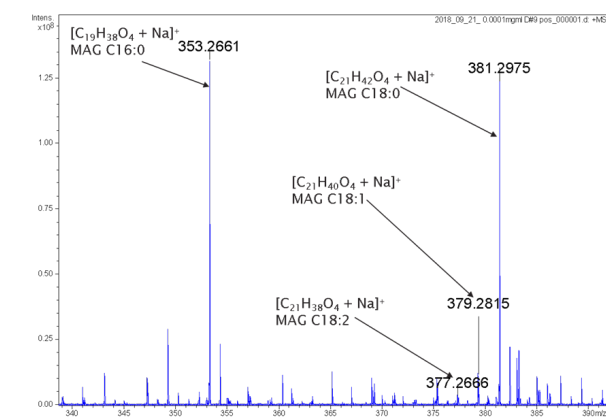

Figure 17   Direct infusion positive ion ESI FT-ICR mass spectrum of diesel 9, (zoomed range m/z 340-390), showing sodiated molecules for MAGs.

As observed previously with FAMEs, nominally isobaric species are also observed between MAGs [C16:0 + Na]$^+$ and [C18:3 + H]$^+$, however for [MAG C16:0 + Na]$^+$ and [MAG C18:3 + H]$^+$ it is at nominal m/z 353 as shown in Table 4. Observation of complimentary adducts and FT-ICR MS analysis allow for separation of isobaric species.

MAGs were observed to be present in diesel 1, 3, 4, 5, 6 and 9 only, with tentative observations by FT-ICR MS only in diesel 2 and diesel 7 (suggesting possibly MAGs absent) and MAGs were found to be absent in diesel 8.
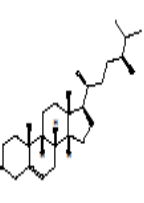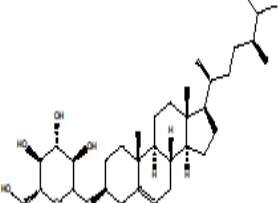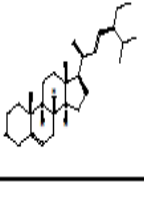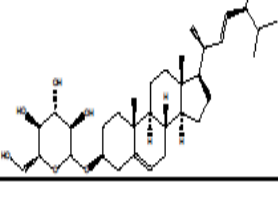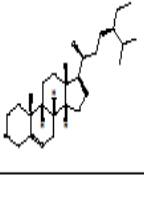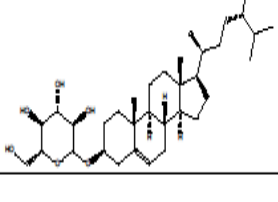
STEROL GLUCOSIDES (SGs)

Sterol glucosides (SGs) consists of a sterol linked at the hydroxyl group (by a glycosidic bond) to a sugar [33]. SGs are present as contaminants, within biodiesel [28].

SGs naturally exist in the acylated form (with a fatty acid attached) in vegetable oil and are converted to SGs during transesterification. The loss of the fatty acid chain reduces the solubility of SGs in biodiesel [34] Cold temperatures and concentration exacerbate the precipitation of SGs, forming large complex agglomerates with MAGs or DAGs in biodiesel and biodiesel blends, resulting in solid residues that can clog fuel filters [28,34].

SGs can cause biodiesel to appear hazy at room temperature due to SGs high MP (*e.g.* 240 °C for β-sitosterol glucoside) that results in limited solubility even at low concentrations (10-90 ppm). Processing is used to reduce SG content to stop related issues, however, low levels can still settle in the bottom of fuel storage tanks and build up over time [34].

Table 5 shows a summary of the SGs, their respective molecular formulae and structures, adducts that can be present and their associated masses [35].

Table 5 SGs Molecular formulae and masses

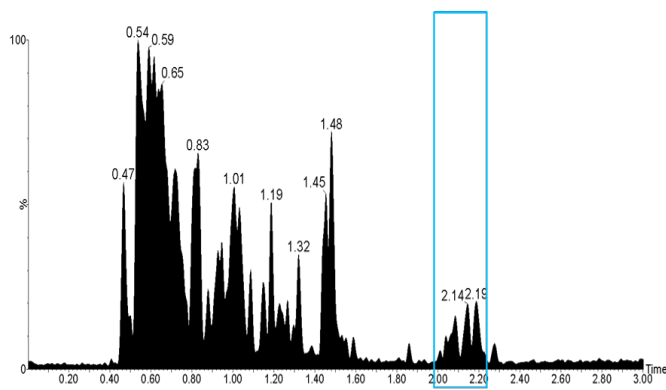| Sterol glucosides	Molecular formula and structure of sterol fragment ion	$[M + H - sugar]^+$	Molecular formula, exact mass and structure of sterol glucoside	$[M + NH_4]^+$ sterol glucoside
			m/z (nominal for UHPSFC-MS, monoisotopic for FT-ICR MS)	
Campesterol glucoside	$C_{28}H_{47}^+$	383.3672	$C_{34}H_{58}O_6$, 562.42 g/mol	580
Stigmasterol glucoside	$C_{29}H_{47}^+$	395.3672	$C_{35}H_{58}O_6$, 574.42 g/mol	592
β-sitosterol glucoside	$C_{29}H_{49}^+$	397.3829	$C_{35}H_{60}O_6$, 576.44 g/mol	594

Figure 18 Positive ion ESI UHPSFC-MS BPICC of diesel3 with pale blue box highlighting SGs region of retention (t_R 2.00-2.20 min.).
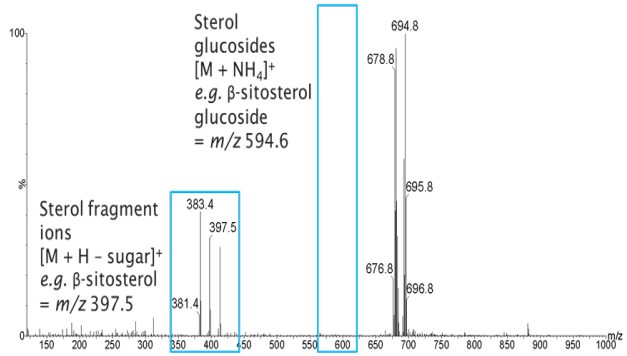

Figure 19 Positive ion ESI UHPSFC mass spectrum of diesel3 at t_R 2.00-2.20 min with pale blue boxes highlighting the *m/z* values expected for SGs and sterol fragment ions

RICCs Figure 20 also confirm that SGs are not present in diesel 3 as the chromatographic peaks for the sterol fragment ion $[M + H - sugar]^+$ and the SG $[M + NH_4]^+$ should be at the same retention time (*e.g.* for campesterol glucoside *m/z* 383 $[M + H - sugar]^+$ and *m/z* 580 $[M + NH_4]^+$). However, no SG peaks are observed at the retention time of interest (2.00-2.20 min) that match with sterol fragment ion, this suggests the absence of SGs (or below LLOD in full scan) in diesel 3 SGs and sterol fragment ions were also not observed by direct infusion positive ion ESI FT-ICR MS.
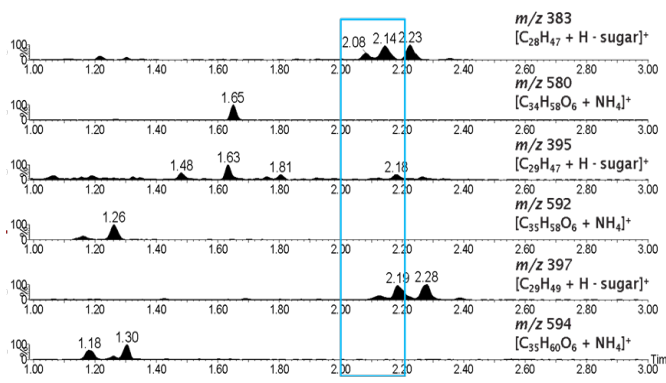
Diesel 3 will be used to illustrate this analysis. SGs have been observed previously in biodiesel blend (unknown diesels) samples by Patel[38]. However, in this case, only the sterol fragment ions were observed in the diesels. Sterol fragment ions (with the absence of SGs) were found to elute at t_R 2.00-2.20 min as shown in Figure 18. The corresponding positive ion ESI UHPSFC mass spectrum Figure 20 shows sterol fragment ions, corresponding to the protonated molecules $[M + H - sugar]^+$ are observed at nominal *m/z* 380-400. However, there is an absence of ammoniated molecules for SGs at nominal *m/z* 580-600 in full scan data. SGs in this case may be present below the lowest limit of detection(LLOD).

Figure 20 Positive ion ESI UHPSFC-MS RICCs of diesel3 showing SGs and sterol fragment ions with pale blue box highlighting SGs region of retention (t_R 2.00-2.20 min.).

SGs were absent in all nine diesels during analysis, as no SG ions were observed relating to relevant sterol fragment ions. This may suggest that processing has taken place to remove SGs to reduce related issues or that SGs are at such low levels they are not detected. It should be noted that the techniques described have detected SGs on filter media [5] so more work may be required to lower the detection limit.

However, sterol fragment ions were observed in diesels 1, 3, 4, 5, 6, 8 and 9, although the stigmasterol fragment ion was only observed in diesel 1. Further investigation showed these fragments were related to fatty acid sterol esters (FASEs).

FATTY ACID STEROL GLUCOSIDES (FASEs)

The presence of the sterol fragment ion was indicative that a sterol related compound was present in all of the fuels except diesel 2 and diesel 7. The possibility of the presence of another plant sterol species was investigated in conjunction with considering a series of chromatographic peaks are present at t_R 2.00-2.40 min Figure 22 and the related positive ion ESI UHPSFC mass spectrum shown in Figure 22.
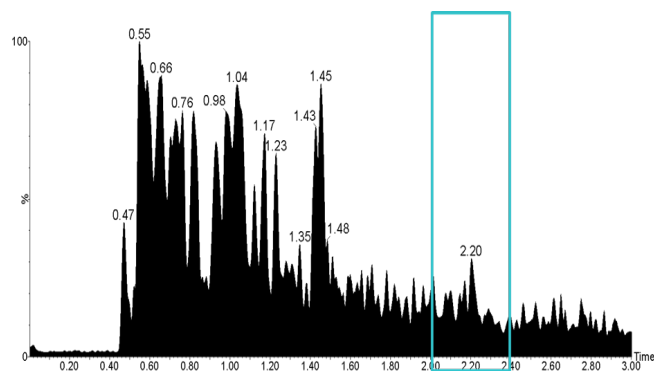

Figure 21 Positive ion ESI UHPSFC-MS BPICC of diesel 1 with pale blue box highlighting FASEs region of retention (t_R 2.00-2.40 min.).
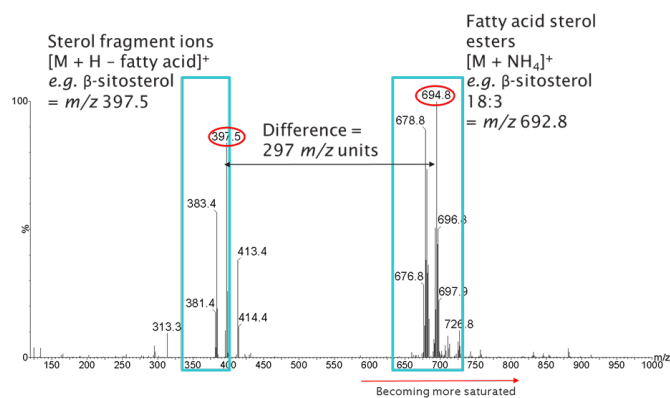

Figure 22 Positive ion ESI UHPSFC mass spectrum of diesel at t_R 2.00-2.40 min with pale blue boxes highlighting the m/z values expected for FASEs and sterol fragment ions

RICCs Figure 23 also confirm that FASEs are likely to be present in diesel 1 as the chromatographic peaks for the sterol fragment ion (*e.g.* campesterol

glucoside m/z 383 [M + H – fatty acid]$^+$ and related FASEs m/z 678, 680 and 682 [M + NH$_4$]$^+$) are at corresponding retention times with chromatographic separation based on degree of saturation of the fatty acid chain.
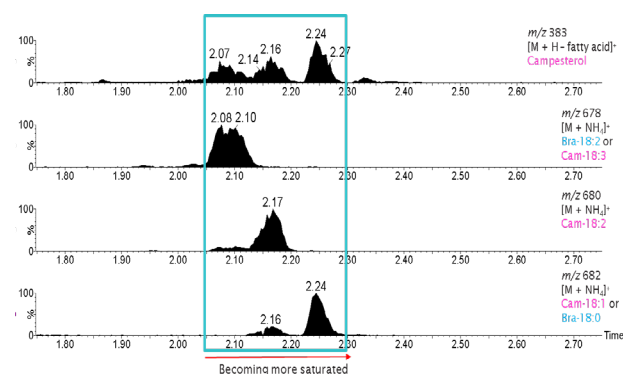

Figure 23 Positive ion ESI UHPSFC-MS RICCS of diesel3 showing campesterol fragment ion and its respective FASEs in with pale blue box highlighting FASEs region of retention (t_R 2.05-2.30 min.).

The observation of FASEs in diesel/biodiesel fuel blends is of significance in the field. As prior to this work, in the literature, FASEs have only been analyzed in pure biodiesel and vegetable oils[37-41] and not in fuel blends Feld and Oberender [42] discussed FASEs as possible contaminants of biodiesel that may form deposits after seed crystals of SGs have initially accumulated in fuel filters.
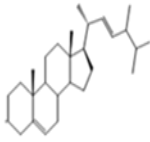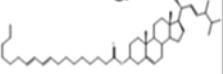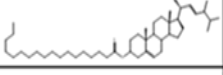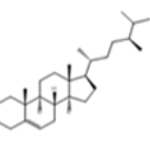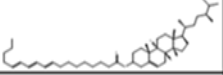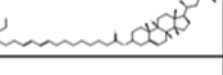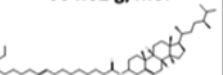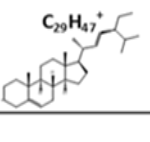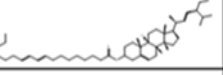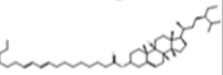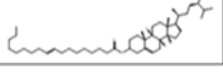
Tandem MS (MS/MS) was undertaken on diesel 1 to characterize the suspected FASEs species further fully within the fuel. The masses for the ammoniated molecules [M + NH$_4$]$^+$ of interest, in this case, m/z 678, 680, 682, 692, 694 and 696 as shown in Table 6, were individually isolated and then fragmented in the collision cell. Four different collision energies were considered; 5, 10, 20 and 30 V, with 10 V being considered the optimal. The resulting product ions were then detected as shown in the example for campesterol esters Figure 24.

The product ion scan for m/z 678 shows that precursor ion m/z 678 has two product ions related to it; m/z 381 and m/z 383. The m/z 381 and m/z 678 ions suggest Brassicasterol ester 18:2 while m/z 383 and m/z 678 suggest Campesterol ester 18:3 is present. As aforementioned, the loss of 297 and 295 m/z units respectively is the loss of fatty acid chains differing by a double bond. This confirms that the sterol fragment ions are product ions of the precursor ions observed, in this case m/z 678.

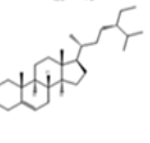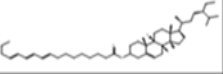The product ion scan for m/z 680 shows that precursor ion m/z 680 has one product ion related to it; m/z 383. From, m/z 383 and m/z 680 suggest Campesterol ester 18:2 is present with the loss of 297 m/z units is the loss of fatty acid chain.

The product ion scan for m/z 682 shows that precursor ion m/z 682 has one product ion related to it; m/z 383. From, m/z 383 and m/z 682 suggest Campesterol ester 18:1 is present with the loss of 299 m/z units is the loss of fatty acid chain.

Table 6 FASEs molecular formulae and masses

| Fatty acid sterol esters	Sub compounds (degree of saturation)	Molecular formula and structure of sterol fragment ion	[M + H − fatty acid]$^+$ sterol fragment ion	Molecular formula, exact mass and structure of sterol ester	[M + NH$_4$]$^+$ sterol ester
Brassicasterol ester	18:02	$C_{28}H_{45}{}^+$	381	$C_{46}H_{76}O_2$ 660.58 g/mol	678 (t$_R$:2.09 min)
	18:00		381	$C_{46}H_{80}O_2$ 664.62 g/mol	682 (t$_R$:2.16 min)
Campesterol ester	18:03	$C_{28}H_{47}{}^+$	383	$C_{46}H_{76}O_2$ 660.58 g/mol	678 (t$_R$:2.09 min)
	18:02		383	$C_{46}H_{78}O_2$ 662.60 g/mol	680 (t$_R$:2.17 min)
	18:01		383	$C_{46}H_{80}O_2$ 664.62 g/mol	682 (t$_R$:2.24 min)
stigmasterol ester	18:02	$C_{29}H_{47}{}^+$	395	$C_{47}H_{78}O_2$ 674.60 g/mol	692 (t$_R$:2.14 min)
β-sitosterol ester	18:03	$C_{29}H_{49}{}^+$	397	$C_{47}H_{78}O_2$ 674.60 g/mol	692 (t$_R$:2.14 min)
	18:02		397	$C_{47}H_{80}O_2$ 676.62 g/mol	692 (t$_R$:2.20 min)
	18:01		397	$C_{47}H_{82}O_2$ 678.63 g/mol	696 (t$_R$:2.29 min)
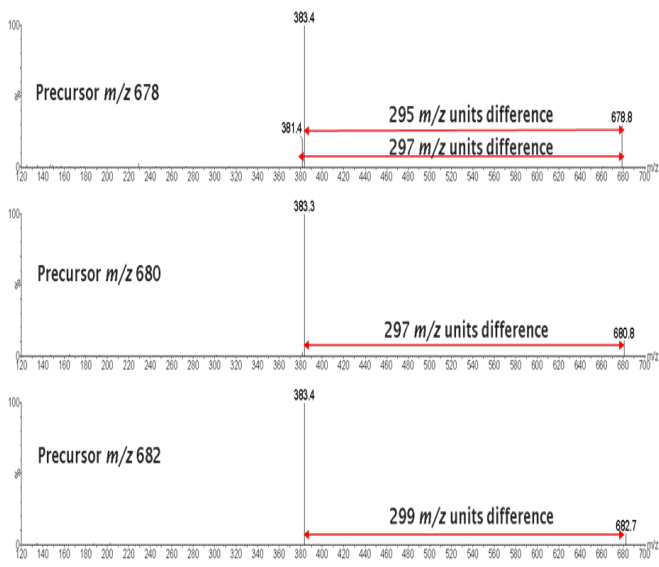
Figure 24 Product ion mass spectrum of diesel 1 of precursors nominal *m/z* 678 (top), 680 (middle) and 682 (bottom) for campesterol esters at t_R 2.28, 2.37 and 2.46 min (TQD) respectively (zoomed over *m/z* 120-700) CE 10V.

FASEs were observed to be present in diesels1, 3, 4, 5, 6, 8 and 9 during analysis. FASEs were found to be absent in diesel 2 and 7.

Stigmasterol ester 18:2 appears to be absent in all fuels with the exception of diesel 3 but that is at low abundance. Campesterol esters and β-sitosterol esters were the most abundant FASEs in the diesel samples.

The presence of FASEs in diesels is believed to be linked to biodiesel and feedstocks so may suggest poor transesterication. In summary

- FAME: Found in all 9 diesels.
- FAME OXIDATION PRODUCTS: Found in all 9 diesels.
- FREE FATTY ACIDS: Found in all 9 diesel fuels.
- MONOACYLGLYCEROLS: observed to be present in diesels1, 3, 4, 5, 6 and 9 only,
- STEROYL GLUCOSIDES: Absent in the 9 diesels.
- STEROLS (fragment ions): Observed in diesels 1,3,4,5,6,8and 9.
- FATTY ACID STEROL ESTERS: Observed in diesels 1,3,4,5,6,8and 9, absent in 2 and 7.

CONCLUSION

A rapid mass spectrometry methodology has been developed to allow the screening of biocomponents implicated in "field" filter and injector problems involving FAME species. originating from FAME in petrodiesel/FAME fuel blends. Thus informing stakeholders in blending regarding the presence of possible problem molecules. This was without expensive/difficult to source standard materials, using minimal sample and without any sample derivatization steps. These methods will be extended in the future to include different mass spectrometry techniques, other filter blocking species and quantitation.

FASEs have been identified in filter blocking residues from petrodiesel/biodiesel blends for the first time. Further, because sterol glucosides and free fatty acids are deposit forming compounds and that acylated sterol glucosides become less soluble in biodiesel upon loss the fatty acid chain during esterification FASEs may be molecules of concern regarding filter blocking.

REFERENCES

1. Zhang, X., Kushner, P.J., Saville, B.A., and Posen, I.D., "Cold Temperature Limits to Biodiesel Use Under Present and Future Climates in North America". Environ. Sci. Technol. 2022,56,8460-8649.
2. Csontos, B., Bernemyr, H., Pach, M., Hittig, H., "Analysis of the Interaction between Soft Particles and Fuel Filter Media". SAE Int. J. Fuels Lubr., 2021, 14 (3), 161-173. DOI: 10.4271/04-14-03-0010.
3. Csontos, B., Berneyer, H., Erlandsson, A.C., Forsburg, O.et al., "Characterization of Deposits Collected from Plugged Filters". SAE Int. J. Adv. & Curr. Prac. in Mobility 2020, no. 2, 672-680. doi:https://doi.org/10.4271/2019-24-0140.
4. Csontos, B., Hittig, H., Pach, M., Bernemyr H. and Erlandsson, A., "A Measurement of Fuel Filters' Ability to Remove Soft Particles, with a Custom-Built Fuel Filter Rig." SAE Technical Paper, 2020, 2020-01-2130.
5. Barker, J., Langley, G., Carter, A., Herniman, J. et al., "Investigations Regarding the Causes of Filter Blocking in Diesel Powertrains"., SAE Technical Paper   2022, 2022-01-1069, doi:10.4271/2022-01-1069.
6. Spanu, M., Barker, J., Reid, J., Scurr, D., and Snape, C., "Detailed Characterization of Diesel fuel Filter deposits by Tof SIMS and other Analytical methods". 12th International Colloquium Fuels Conventional and Future Energy for Automobiles,2019, 25-26 June. Technische Akademie Esslingen Stuttgart/Ostfildern.
7. Fersner, A.S. and Galante-fox, J.M. "Biodiesel Feedstock and Contaminant Contributions to Diesel Fuel Filter Blocking". SAE Int J Fuel and Lubr., 2014, 7,783-791.
8. American Society for Testing and Materials. "Standard Test Method for Determining Filter Blocking Tendency".ASTM   D2068-20. West Conshohocken PA. USA.
9. Jolly, L., Kitano, K., Sakata, I., Strojekw W., et al. "A Study of Mixed FAME and Trace Component Effects on the Filter Blocking Propensity of FAME and FAME". SAE Technical Paper, 2010 2010-01-2116, doi:10.4271/2010-01-2116.
10. Goplan, K., Chuck, C.J., Roy-Smith, C. and Bannister C.D., "Assessing the Impact of FAME and Diesel Fuel Composition on Stability and Vehicle Filter Blocking". SAE Int. J. Adv in Curr. Prac. Mobility, 2019,1, 284-290. doi:10:4271/2019-01-0049
11. Barker, J., Richards, P., Snape, C., and Meredith, W., "Diesel Injector Deposits an Issue That has evolved with Engine Technology". SAE Technical Paper 2011, 2011-01-1923, doi:10.4721 2011-01-1923.
12. Richards, P., Barker, J., Cook, S., "Addressing the Issue of Fuel Filter Fouling with recent Changes in Fuel Quality"., J. ASTM Int.2009 6, 10-14
13. Heiden, R.W., Schrober, S., "Solubility Limitations of Residual Steryl Glucosides, Saturated Monoglycerides and Glycerol in Commercial Biodiesel Fuels as Determinants of Filter blockages". J. Am. Oil Chem. Soc. 2021, 98, 1143-1165.
14. European Committee for Standardization "Liquid Petroleum Products -Fatty Acid Methyl Esters (FAME) for use in Diesel Engines and Heating Applications Requirements and Test Methods-EN14214 :2012+A2:2019
15. American Society for Testing and Materials "Standard Specification for Biodiesel Fuel Blend Stock (B100) for Middle Distillate Fuels", D6751-23a. West Conshohocken PA. USA.
16. European Committee for Standardization "Automotive fuels and fat and oil derivates - Determination of saturated monoglycerides content in Fatty Acid Methyl Esters (FAME) - Method by GC-FID". EN 17057: 2018.
17. Barker, J., Reid, J., Smith, S.A., Snape, C., Scurr, D., Langley, G., Patel, K., Carter, A., Lapthorn, C., Pullen, F., "The application of new approaches to the analysis of deposits from the Jet Fuel Thermal Oxidation Tester (JFTOT)". SAE Int. J Fuels and Lubr., 2017,10, 3, 741-755.
18. Barker, J., Langley, G., and Richards, P., "Insights into deposit formation in high pressure diesel fuel injection equipment". SAE Technical Paper 2010, 2010-01-2243
19. Barker, J., Cook, S., and Richards, P., Sodium Contamination of Diesel Fuel, its Interaction with Fuel Additives and the Resultant Effects on Filter Plugging and Injector Fouling. SAE Int. J. Fuels Lubr. 2013, *6* (3), 826-838
20. Ratsameepakai, W.; Herniman, J. M.; Jenkins, T. J.; Langley, G. J.," Evaluation of Ultrahigh-Performance Supercritical Fluid Chromatography–Mass Spectrometry as an Alternative Approach for the Analysis of Fatty Acid Methyl Esters in Aviation Turbine Fuel." Energy & Fuels 2015, *29* (4), 2485-2492.
21. Bannister, C. D.; Chuck, C. J.; Bounds, M.; Hawley, J. G., "Oxidative Stability of Biodiesel Fuel." Proceedings of the Institution of Mechanical Engineers, Part D: Journal of Automobile Engineering 2011, *225* (1), 99-114.
22. Bondioli, P.; Gasparoli, A.; Lanzani, A.; Fedeli, E.; Veronese, S.; Sala, M., "Storage stability of biodiesel." Journal of the American Oil Chemists' Society 1995, 72 (6), 699-702.
23. Lacey, P.; Gail, S.; Kientz, J.; Benoist, G.; Downes, P.; Daveau, C., "Fuel Quality and Diesel Injector Deposits." SAE Int. J. Fuels Lubr. 2012, 5 (3), 182-195.
24. Urzędowska, W.; Stępień, Z., "Prediction of threats caused by high FAME diesel fuel blend stability for engine injector operation." Fuel Process. Technol. 2016, 142, 403-410
25. Alberici, R. M.; de Souza, V.; de Sá, G. F.; Morelli, S. R.; Eberlin, M. N.; Daroda, R. J., "Used Frying Oil: A Proper Feedstock for Biodiesel Production?" Bioenergy Research 2012, 5 ,4, 1002-1008.
26. Trobaugh, C., Burbrink, C., Zha, Y., Whitacre, S. et al., "Internal Diesel Injector Deposits:

Theory and Investigations into Organic and Inorganic Based Deposits." SAE Int. J. Fuels and Lubr. 2013, 6, 772-784.

27. IUPAC., Compendium of Chemical Terminology (the "Gold Book"). 2nd ed.; McNaught, A. D.; Wilkinson., A.; Chalk., S. J., Eds. Blackwell Scientific Publications: Oxford, 1997.

28. Dunn, R. O., "Effects of Minor Constituents on Cold Flow properties and Performance of Biodiesel". Prog. Energy Combust. Sci. 2009, 35, 6, 481-489.

29. Kortba, R., "Bound by Determination". Biodiesel Magazine 2006, October pp 42-50. Accessed March 2022.

30. Dunn, R. O., "Effects of Monoacylglycerols on the Cold Flow Properties of Biodiesel". J. of the Am. Oil Chem. Soc. 2012, 89 ,8, 1509.

31. Knothe, G.; Krahl, J.; Van Gerpen, J., Eds "Fuel Properties". The Biodiesel Handbook (Second Edition). AOCS Press: 2010; pp 137-251.

32. Kalo, P. J.; Ollilainen, V.; Rocha, J. M.; Malcata, F. X., "Identification of molecular species of simple lipids by normal phase liquid chromatography–positive electrospray tandem mass spectrometry, and application of developed methods in comprehensive analysis of low erucic acid rapeseed oil lipids ". Int. J. Mass Spectrom. 2006, 254 ,1, 106-121

33. Hoed V., Zyaykina, N., Greyt, W., Maes, J., Vehre,J., Demeestere, K., "Identification and Occurrence of Sterol Glucosides in Palm and Soy Diesel". J. Am. Oil Chem. Soc. 2008, 85,

34. Lee, I., Pfaltzgraf, L.M., Poppe, G.B., Powers E., Haines, T., "The Role of Sterol Glucosides on Filter Plugging". Biodiesel Mag. April (2007), http:/www.biodiesl magazine.com/articles/1566/the-role-of- sterol-glucosides-on-filter-plugging ". Accessed March 2023

35. Oppliger, S.; Munger, L.; Nystroem, L., "Rapid and Highly Accurate Detection of Stearyl Glucosides by Ultraperformance Liquid Chromatography/Quadrupole Time of Flight Mass Spectrometry ". J. Agric. Food. Chem. 2014, 62 ,4.

36. Wewer, V.; Dombrink, I.; vom Dorp, K.; Dörmann, P., "Quantification of Sterol Lipids in Plants by Quadrupole Time-of-flight Mass Spectrometry". J. Lipid Res. 2011, 52 ,5, 1039-1054.

37. Patel K Doctoral Thesis University of Southampton 2016.

38. Hailat I, Helleur E.T.R., "Identification of Fatty Acid Steryl Esters in Margarine and Corn Using Direct Flow Injection ESI MS Ion-Trap Mass Spectrometry". Int. J. Mass Spectrom. 2014, 362, 24-31.

39. Plank, C., Lorbeer, E. "On-line liquid Chromatography Gas Chromatography for the Analysis of Free and Esterified Sterols in Vegetable Oil Methyl Esters used as Diesel Fuel Substitutes". J. Chromatogr. A, 1994, 683 ,1,95-104

40. Plank, C., Lorbeer, E., "Minor Components in Vegetable Oil Methyl Esters I: Sterols in Rape Seed Oil Methyl". Lipid/Fett 1994, 96, 10, 379-386

41. Verylen, T., Forcades, M., Verhe, R., Dewettinck, K., Huyghebaert, A., De Greyt W. C., "Analysis of Free and Esterified Sterols in Vegetable Oils". J. of Am. Oil Chem. Soc., 2002 79,2,177-122.

42. Feld, H., Oberender, N ., "Characterization of Damaging Biodiesel Deposits and Biodiesel Samples by Infrared Spectroscopy (ATR-FTIR) and Mass Spectrometry (TOF-SIMS)". SAE Int. J. of Fuels and Lubr., 2016, 9, 717-724. https://doi.org/10.4271/2016-01-9078

CONTACT

Dr. Jim Barker
Tel: +44 151 355 3611
Email: jim.barker@Innospecinc.com

Innospec Limited
Innospec Manufacturing Park
Oil Sites Road
Ellesmere Port
Cheshire, CH65 4EY
England

http://www.innospecinc.com